
Quantitative Measurement of Myocardial Blood Flow with Oxygen-15 Water and Positron Computed Tomography: An Assessment of Potential and Problems

S. C. Huang, M. Schwaiger, R. E. Carson, J. Carson, H. Hansen, C. Selin, E. J. Hoffman, N. MacDonald, H. R. Schelbert, and M. E. Phelps

Division of Nuclear Medicine and Biophysics, Department of Radiological Sciences, UCLA School of Medicine, and Laboratory of Nuclear Medicine, University of California, Los Angeles, California

An in vivo measurement technique using ^{15}O water and positron CT for quantitation of myocardial blood flow (MBF) was investigated. A closed-chest dog model and NeuroECAT[†] scanner were used in the study. The in vivo technique involves i.v. infusion of ^{15}O water for a duration of 2–3 min. Oxygen-15 water radioactivity in myocardium was imaged with a NeuroECAT scanner for 10 min, starting at the time of tracer infusion. A separate scan following inhalation of ^{15}O CO was obtained to label the blood pool and to help remove the contribution of radioactivity in the blood pool during the ^{15}O water scans. The integrated projection technique was used for calculating MBF. The quantitative microsphere technique for measurement of MBF was performed along with the ^{15}O water study to provide reference values, with which the MBF values by the in vivo technique were compared. Results of 12 experimental runs (in seven animals) show the in vivo technique with ^{15}O water and positron CT can give quantitative flow images of myocardium. The in vivo positron CT measurement was found to correlate well ($r = 0.93$) with the in vitro values (by microspheres) over the flow range of 40 to 150 ml/min/100 g.

J Nucl Med 26:616–625, 1985

Positron computed tomography (CT) can provide quantitative measurements of physiological processes noninvasively, if suitable tracers are used and if appropriate mathematical models are formulated (1–3). For the measurement of regional myocardial blood flow (MBF) with positron CT, the tracer nitrogen-13 (^{13}N) ammonia has been carefully examined in dogs (4) and used in man with good results for delineating ischemic myocardium (5). However, because of the incomplete single-pass extraction of ammonia by myocardium and the appearance of ^{13}N amino acids in plasma, in vivo quantitation of MBF with [^{13}N]ammonia is difficult,

although not impossible (6). Further, [^{13}N]ammonia is trapped metabolically in tissue, thus raising the criticism that uptake of [^{13}N]ammonia may be modified by factors other than blood flow alone (7).

Oxygen-15 water has been successfully employed for measurements of local cerebral blood flow (CBF) in man using positron CT (8–12). Because ^{15}O water is also freely diffusible across membranes of myocardium (13), the tracer should be applicable for measurement of MBF. The tracer ^{15}O water has been used with positron CT to evaluate the relative distribution of MBF (14). Allen et al. (15) have also used continuous inhalation of ^{15}O CO₂ and the equilibrium technique (16) to measure MBF. The technique appears promising, but results have not been reported in full detail.

Some potential difficulties that are unique to the positron CT studies of the heart need to be overcome

Received June 22, 1984; revision accepted Mar. 13, 1985.

For reprints contact: Sung-cheng Huang, DSc, Div. of Nuclear Med. and Biophysics, Dept. of Radiological Sciences, UCLA School of Medicine, 405 Hilgard Ave., Los Angeles, CA 90024.

before MBF can be measured in ml/min per gram of myocardium with the ^{15}O water technique. The major problems are related to (a) the blood-pool activity in the cardiac chambers; (b) the relatively thin walled myocardium; and (c) the motion of the heart. The partial volume effect associated with the relatively thin-walled myocardium and the cardiac motion problem are common to all positron CT studies of the heart and have been discussed and studied extensively before (17–19). Usually, the blood-pool spillover can be corrected by the use of ^{15}O CO to label the blood pool for subtraction of radioactivity in the cardiac chamber (14,15). However, the possible errors from this subtraction technique for ^{15}O water studies have not been evaluated systematically.

Except for the equilibrium technique, the tracer is usually administered as a rapid bolus. The fast transit of the bolus through the cardiac chambers in the imaging plane could cause high count rates that exceed the capability of most positron CT scanners (20) and would produce serious image artifacts for nonstationary type scanners (21,22). This problem can be reduced if ^{15}O water is injected slowly (i.e., a distributed bolus). The integrated projection technique (23) which allows complete flexibility for the input function and thus for the administration of ^{15}O water is ideal for this purpose. In this paper, we report the use of the above method in dogs to examine the feasibility of using ^{15}O water and positron CT for quantitative measurement of MBF. The measurements were compared to those by radiolabeled microspheres and the arterial reference sampling technique (4,24).

MATERIALS AND METHOD

Production of ^{15}O CO and ^{15}O water

Oxygen-15 CO and ^{15}O water were produced by the UCLA medical cyclotron[†] as described previously (25,10).

Animal preparation

Seven mongrel dogs (18–24 kg) were anesthetized with sodium pentobarbital (25 mg/kg) and ventilated with room air. Catheters were advanced into the femoral vein and artery for injection of the radioactive tracer and for arterial blood sampling. After left thoracotomy, a catheter was inserted into the left atrium for injection of microspheres. An electromagnetic flow probe[§] was placed around the proximal circumflex artery to monitor changes in coronary blood flow. Following instrumentation, the chest was closed and the animal positioned into the tomograph. Arterial blood pressure, electrocardiogram, and the flow probe signal were recorded continuously on a strip chart recorder.[¶]

Study protocol

The animal was placed supine in a NeuroECAT scanner (20). A rectilinear transmission scan was obtained and used for positioning the imaging plane through the mid left ventricle. A transmission scan was then obtained. Oxygen-15 CO gas (about 30 mCi) was introduced to the animal through a respirator. One and a half minutes later, a 2-min scan of the blood-pool activity was initiated. At mid time of the scan, an arterial blood sample was taken and counted in a well counter to provide a direct calibration for the concentration of ^{15}O CO in the positron CT image.

Oxygen-15 water (about 50 mCi in 3–4 ml) was then infused into the femoral vein catheter with a Harvard pump at a rate of 1.5 ml/min. Beginning with the infusion, five 2-min positron scans were acquired and serial arterial blood samples were withdrawn over a 10-min period (at a rate of 5/min for 2.5 min, followed by 2/min for 2 min, and 1/min and 2/min until end). The ^{15}O activity in blood samples was immediately determined in a well counter. Between 3 to 5 min prior to administration of ^{15}O water, gamma-emitting microspheres were injected into the left atrium. Microsphere MBF was used as a reference against which MBF calculated *in vivo* by the ^{15}O water method was compared.

The above ^{15}O water injection and scanning procedure was usually repeated in the same dog after MBF was increased with dipyridamole (i.v. infusion rate of 0.07 mg/min/kg for 4 min) or reduced with morphine sulfate (0.5–1.5 mg/kg).

Positron CT scanning and data processing

The “septa in,” “shadow shield in,” and “high sampling mode (sampling space of 0.2775 cm)” options (20) of the NeuroECAT were selected for the studies. The low resolution filter was used for CT image reconstruction. With these selections, image resolution is 1.2 cm full width at half maximum (FWHM) (20). Photon attenuation was corrected for from measurements of the transmission scan taken at the beginning of the study. Calibration between the positron CT scanner and the well counter was done for each study as previously described (26,27).

The NeuroECAT software system was modified beforehand to save the unsorted scan data and their exact collection time during the ^{15}O CO and ^{15}O water scans, similar to the approach employed for measurements of CBF with ^{15}O water (10). These data were normalized for variations in detector efficiency and sorted into time functions for all the projection measurement positions. The fraction of radioactivity due to the ^{15}O water in the blood pool was removed by subtracting the projection measurements of the ^{15}O CO scan from the corresponding projections of the ^{15}O water scans according to the following equation

$$m_c(r, \theta, t) = m_w(r, \theta, t) - m_{co}(r, \theta) * C_i(t) / C_{co} \quad (1)$$

where $m_w(r, \theta, t)$ is the projection measurement of the water scans at location (r, θ) , t is the time of the measurement, m_{co} is the corresponding projection measurement of the CO scan, C_{co} is the radioactivity concentration of the blood sample taken at the mid time of the CO scan, $C_i(t)$ is the ^{15}O water concentration of the blood time-activity curve (linearly interpolated from the blood samples taken during the ^{15}O water scans) at the time of the projection measurement time t , and m_c is the resulting projection measurement from ^{15}O water after removal of ^{15}O radioactivity in blood.

The time functions of the projection measurements ($m_c(r, \theta, t)$) were integrated from time zero (injection time) to time T (about 9 min) (time between the 4th and the 5th scans). The integrations were performed twice—once with and once without decay correction to the beginning time of tracer infusion. The time integrated projections were then used to reconstruct the images of the integrated activities ($\int Q \, dt$ and $\int Q^* \, dt$ in Eq. 2) in the cross-sectional slice by the regular filtered backprojection reconstruction program of NeuroECAT. The images of blood flow (F) and water distribution volume (V) were calculated from these integrated activity images (on a pixel-by-pixel basis) according to the following equations (10)

$$F = \frac{\lambda \int Q^* \, dt \int Q \, dt - Q^*(T) \int Q \, dt}{\int C_i \, dt \int Q^* \, dt - \int Q \, dt \int C_i^* \, dt}$$

$$V = \frac{\lambda \int Q^* \, dt - Q^*(T)}{\lambda \int C_i^* \, dt - Q^*(T) \int C_i \, dt / \int Q \, dt} \quad (2)$$

where λ is the physical decay constant of ^{15}O , C_i is the time-activity curve of ^{15}O in arterial blood as obtained from the arterial blood samples, and the integrations are from time 0 to T . The symbols with asterisk indicate decay-corrected quantities (i.e., decay-corrected to the beginning time of infusion), while those without asterisk are not decay-corrected. The term Q is the ^{15}O radioactivity in tissue. The average image value over the myocardium in the 4th and the 5th scans was used for $Q^*(T)$. The calculation of Eq. (2) was performed only on the pixels that were within the region of the myocardium, as determined from the transmission image and the ^{15}O CO blood-pool image.

Circular regions of interest (ROI), 1.0 cm in diam, were assigned to myocardium on the flow image for calculating the average MBF values within each ROI. Usually, one ROI was placed on the interventricular septum and one on the free left ventricular wall (i.e., the anterior, lateral, or posterior wall). The exact locations of the ROIs were selected on the thickest part of the myocardial wall (judged by the shape and by the activity level on the images of the integrated activities $\int Q \, dt$) to minimize the partial volume effect (17). The same ROIs

were applied to the distribution volume images to obtain the value of distribution volume of water.

In vitro measurement of reference MBF

Reference MBF measurements were obtained with radioactive microspheres and the arterial reference sampling technique (4,24). Gamma-emitting microspheres ($15 \, \mu$)** were injected into the left atrium. Starting at the time of microsphere injection, arterial blood was withdrawn with a Harvard pump at a rate of 4.9 ml/min for 2 min. For multiple experimental runs on the same dog, microspheres labeled with different isotopes (scandium-46, cobalt-57, tin-113) were used. At the end of the experiment, the animal was killed and the heart removed. A 1-cm-thick cross section of the left ventricle that corresponded approximately to the tomographic image plane (marked on the animal's chest according to the low-power positioning laser light of the tomograph) was removed. It was divided into about 1 g samples which were then weighed, and their radioactivities determined in a well counter. MBF was then calculated using the arterial reference sample technique (4). The microsphere MBF in the segment that matched the ROI location selected on the flow image was compared with the MBF value calculated by the ^{15}O water technique.

RESULTS

Figure 1 shows an example of a cross-sectional image



FIGURE 1
Blood-pool image (using ^{15}O CO) of cross section of chest of dog. Sections of left ventricle, vena cava, and aorta are clearly seen. Right ventricle also appears in image, although not as clearly

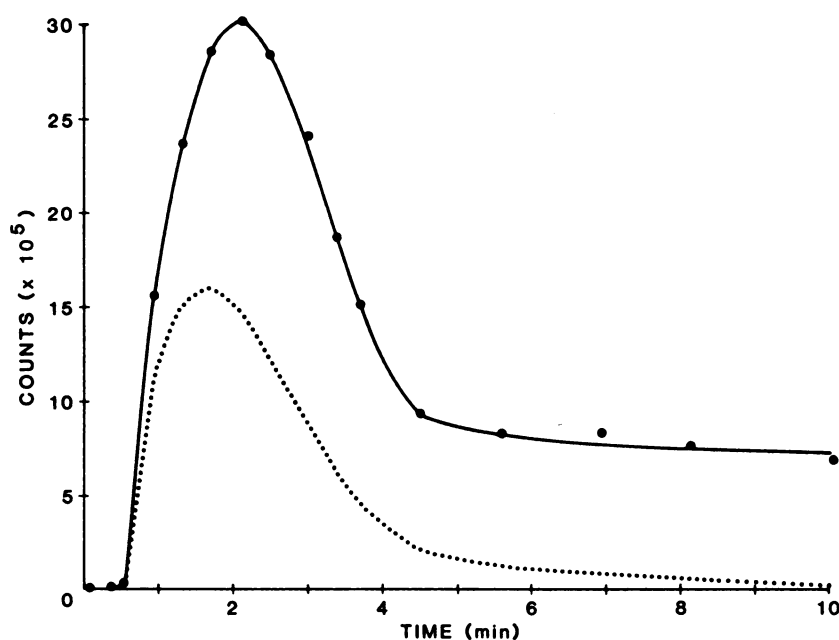


FIGURE 2
Time-activity curve of ^{15}O water in arterial blood in typical study. ^{15}O water was infused i.v. over duration of 2.5 min. Solid line represents radioactivities that have been decay-corrected to time zero (i.e., to beginning of tracer infusion), while dotted line is for nondecay-corrected radioactivities (i.e., decay-corrected only to time of sampling of arterial blood). Integrals of both curves were used in operational equation [Eq. (2)] for calculation of MBF and distribution volume of water

of the blood pools of the heart obtained with ^{15}O CO. This image was used to remove the ^{15}O water activity in the blood pools on the ^{15}O water images.

The time-activity curve of ^{15}O water in blood is shown in Fig. 2. Both the curves before and after correction for decay are shown. Figure 3 shows the regularly reconstructed positron CT images of the five 2-min sequential scans after the start of ^{15}O water infusion. The tracer is present mainly in the blood pools at the beginning of the infusion. With time, the tracer diffuses into tissue. Because of the short half-life of ^{15}O (123 sec), the late scans were low in counts, which accounted for the high noise level of the late images. Figure 4 shows images of the integrated myocardial radioactivities (i.e., $\int Q \, dt$ and $\int Q^* \, dt$) of the study. Images of blood flow and distribution volume of water as calculated by Eq. (2) are shown in Fig. 5. The locations of the ROIs selected are also depicted in the figure.

Coronary blood flow velocity, monitored with the electromagnetic flow probes was usually stable during the experiments except for two studies, when flow velocity between the injection times of microspheres and ^{15}O water changed. In these two studies (D495R2, D495R3), the microsphere flow was adjusted by -33 and 13% according to the percent changes of the flow probe recording between the microsphere and ^{15}O water injection. In two other studies (D475R1 and R2), the MBF value for the septum as calculated from the MPF images exceeded the upper limit of $200 \text{ ml/min}/100 \text{ g}$ preset for the calculation in the computer program. These two studies also contained the largest right ventricle in the image plane among the studies performed.

The values of MBF and distribution volume obtained

in 12 studies are listed in Table 1, along with the MBF value by the microsphere technique. Figure 6 shows the relationship between the positron CT and microsphere MBF values. Curve fitting with polynomial showed that the relationship between the values of the two measurement techniques can be described by (PCT MBF) $= 0.43 + 0.76$ (Microsphere MBF) ($r = 0.89$) for myocardium of the free left ventricular wall, (PCT MBF) $= -6.0 + 0.87$ (microsphere MBF) ($r = 0.93$) for the interventricular septum, and (PCT MBF) $= -1.3 + 0.79$ (microsphere MBF) ($r = 0.93$) for all measurements. Statistical tests (F test (28) with $p = 0.05$) show that none of the data set support a second order polynomial curve fit.

DISCUSSION

Oxygen-15 water has been used with positron CT to examine qualitatively the relative distribution of MBF in ischemic and reperfused myocardium (29). The need of quantitation of MBF is well recognized. The present study indicates that this is possible with the ^{15}O water technique. However, the accuracy and reliability of the quantitative measurements depend on several factors that are discussed below.

Administration of ^{15}O water and measurement of blood radioactivity

In the present study, ^{15}O water was infused i.v. over a time period of 2 to 3 min to avoid the fast transit of a high concentration of ^{15}O water through the heart chambers that a rapid bolus injection would produce. However, the rate and duration of infusion selected in the present study have not been optimized in terms of the

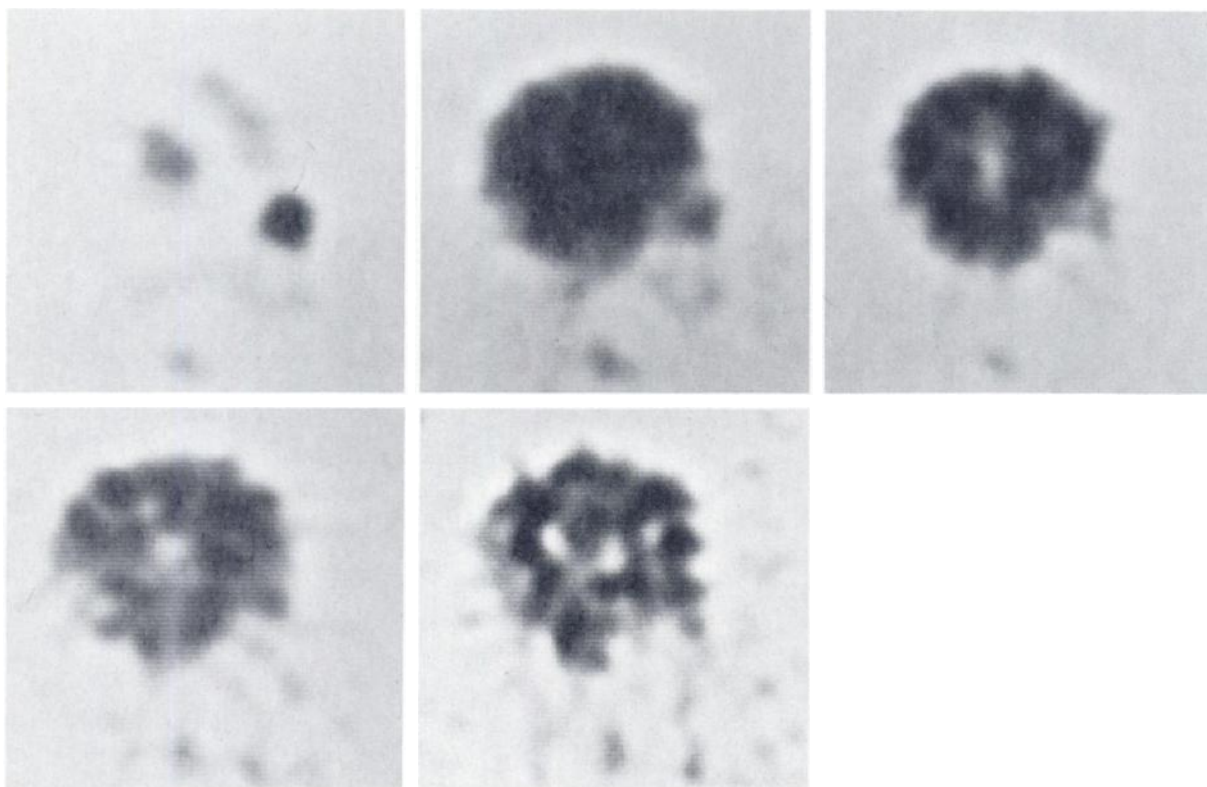


FIGURE 3

Sequence of five 2-min positron CT images of ^{15}O water radioactivity in same cross section as in Fig. 1, after start of infusion of ^{15}O water. Initially, most radioactivity was in blood and thus resembled blood-pool image of Fig. 1. Because the tracer was introduced i.v. and physical decay half-life is short (2 min), vena cava had highest activity. As compared to Fig. 1, right ventricle also showed higher activity. However, as time goes on, ^{15}O water began to diffuse into myocardium tissue. Later, ^{15}O water in blood was cleared faster than in tissue, and showed lower activity in cardiac chamber (3rd and 4th images). Gradually, ^{15}O water distribution in tissue and blood would approach equilibrium state, in which activity ratio between tissue and blood would equal distribution volume (partition coefficient) of water in myocardium. Due to short half-life of ^{15}O , noise level in late images is high

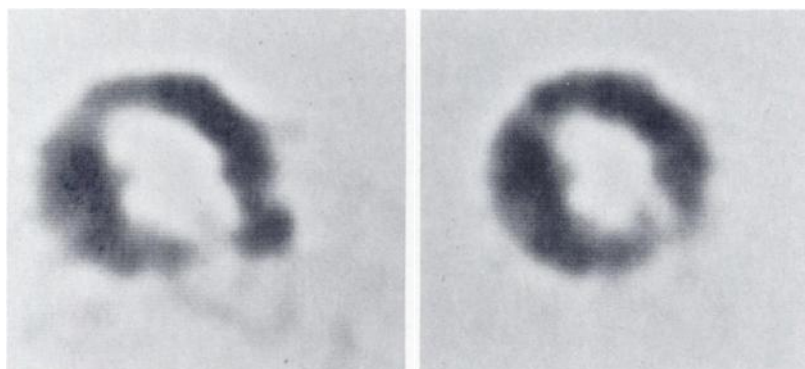
signal-to-noise ratio of the images or the radiation dosage to the studied subject. Optimization of these factors is a complicated problem and depends on the specific positron CT scanner used. This problem is currently being examined systematically in our laboratory.

Measurements of blood flow with this technique usually require arterial blood sampling to provide the

time-activity curve of ^{15}O water in blood. Because the cardiac chambers are usually in the image plane, the radioactivity concentration in blood could also be obtained directly from the serial images, especially for the flow calculation used in the present study which only requires the integrals of the blood-activity curve. This possibility was examined by integrating the time func-

FIGURE 4

Images of integrated radioactivities of Fig. 3. The radioactivities due to ^{15}O activity in blood pools was eliminated according to Eq. (1) before images were reconstructed. Image on left corresponds to integral of nondecay-corrected radioactivities; image on right corresponds to integral of decay-corrected radioactivities. Image scalings of two images were different (see Table 2 for their relative magnitudes)



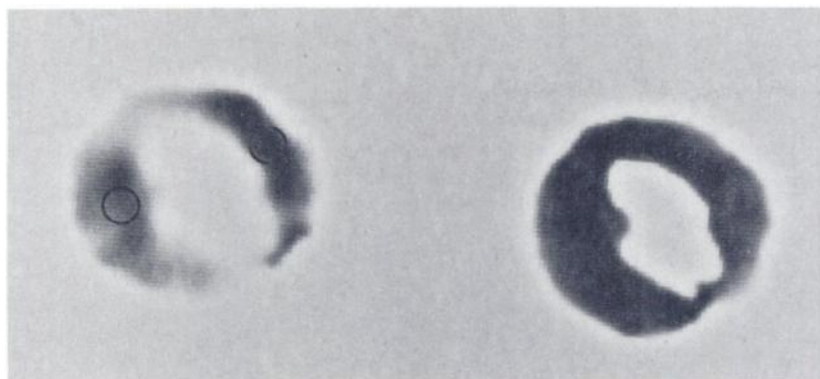


FIGURE 5

Images of MBF (left) and water distribution volume (right) as obtained according to Eq. (2) from the images of Fig. 4 and integrals of blood curves in Fig. 2. Higher value on septum in the MBF image is believed to be due to spillover activity in right ventricle that was not removed completely by blood-pool subtraction technique [Eq. (1)]. (See text for more discussion)

tions of the projection measurements (without subtraction of blood-pool activity) and reconstructing the images of the integrated radioactivities. Images of both the decay-corrected and the nondecay-corrected activities were reconstructed. Radioactivity levels in the cardiac chambers of these images were calculated from an ROI of diameter 1.0 cm at the center of the chamber (as determined from the ^{15}O CO blood-pool image). Table 2 shows the values of the blood curve integrals compared with those from the cardiac chamber of these images ($Q_b Q_b^*$). The smaller values of the integrals obtained from positron CT can be explained by the partial volume effect, which also affects the normalized blood-pool activity (next to last column in Table 2) of the ^{15}O CO blood-pool image.

The spillover of radioactivity from myocardium to the cardiac chamber can account for the slightly larger ratio

of $\int Q_b^* / \int Q_b$ than the one from the blood curve (because the ratio is larger in myocardium than in the blood pool). Normally, the value in the last column of Table 2 should always be larger than one, unless there is a timing delay in the blood curve C_i . For example, if the blood sampling times were delayed by 10 sec, the ratio in the last column of Table 2 would be reduced by about 7%. This property can be used to check whether any timing delay is introduced in measuring the blood curve.

Subtraction of blood-pool activity in the heart chambers

Logically, use of ^{15}O CO to image the blood pool and subtracting it from the ^{15}O water images corrects for spillover activity from the cardiac chambers to myocardium. This approach is, however, associated with a

TABLE 1
Comparison of MBF Values from ^{15}O Water Technique and from Microsphere Technique

| Study no. | ^{15}O water | | | | Microsphere | |
|-----------|-----------------------|--------|--------|--------|-------------|--------|
| | Free wall | | Septum | | Free wall | Septum |
| | MBF* | V* | MBF | V | MBF | MBF |
| D407R1† | 69 | 0.71 | 56 | 0.66 | 106 | 104 |
| D451R1 | 45 | 0.82 | 48 | 0.79 | 54 | 55 |
| D451R2 | 30 | 0.83 | 36 | 0.79 | 42 | 39 |
| D455R1 | 58 | 0.89 | 40 | 0.85 | 68 | 60 |
| D457R1 | 84 | 0.61 | 98 | 0.63 | 133 | 120 |
| D457R2 | 92 | 0.62 | 128 | 0.67 | 152 | 137 |
| D460R2 | 79 | 0.66 | 58 | 0.74 | 97 | 89 |
| D475R1 | 76 | 0.79 | —‡ | — | 96 | 117 |
| D475R2 | 111 | 0.81 | — | — | 143 | 129 |
| D495R1 | 56 | 0.72 | 50 | 0.71 | 75 | 56 |
| D495R2 | 39 | 0.71 | 35 | 0.71 | 63 | 47 |
| D495R3 | 148 | 0.67 | 118 | 0.68 | 146 | 133 |
| Average | 73.9 | 0.74 | 66.7 | 0.72 | 97.9 | 90.5§ |
| (s.d.) | (32.9) | (0.09) | (34.7) | (0.07) | (38.5) | (37.1) |

* MBF values are in ml/min/100 g and distribution volume of water are in ml/g.

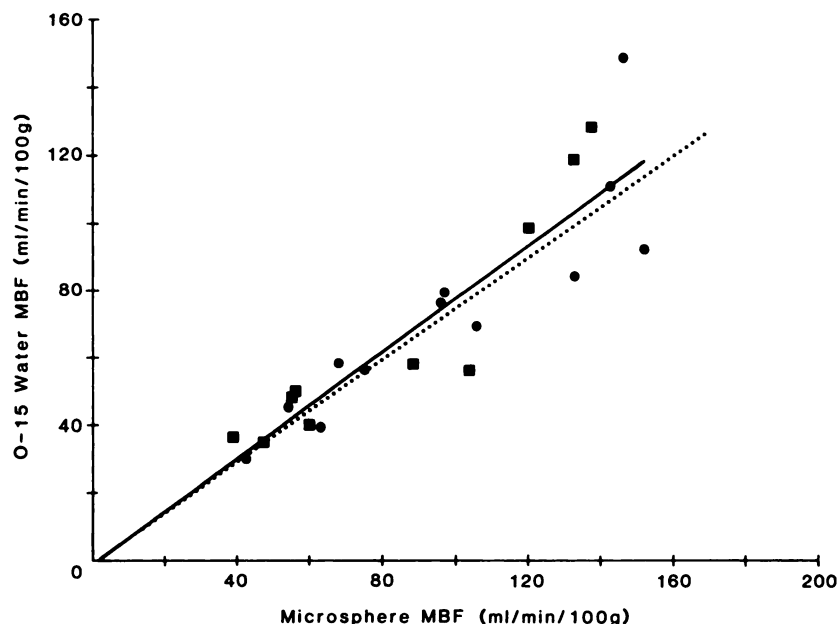
† For all experimental runs on the same animal, the same transmission scan and the same blood pool scan were used.

‡ Calculated MBF exceeded the upper limit of 200 ml/min/100 g preset for the computation in the computer program.

§ The average is 84.0 if values of D475R1 and R2 are not included.

FIGURE 6

Relationship between MBF values of ^{15}O water technique and microsphere technique. Data points shown include those on left ventricular wall (●) and on interventricular septum (■) (except two data points discussed in text and in Table 1). Solid line is linear regression line for all data points in figure ($y = -1.3 + 0.79x$); dotted line is regression for data on left ventricular wall alone ($y = 0.43 + 0.76x$)



number of practical problems. For example, positional changes of the heart between the ^{15}O CO and the ^{15}O water image acquisitions will introduce errors in the subtraction procedure. In the present studies, only one ^{15}O CO blood-pool image was acquired in each animal at the beginning of the experiments. In addition to the relatively long time interval between the blood-pool and the ^{15}O water studies, interventions to alter MBF may have also affected the heart's geometry and imposed additional errors on the subtraction process. This problem can be reduced if ^{15}O CO studies are performed for each intervention state. However, maintaining the intervention states stable for a prolonged time period is difficult, and the total experimental time would also be greatly increased.

The adequacy of blood-pool subtraction can be examined by calculating the ratio of the image values in the left ventricular cavity to that in myocardium on the blood-pool subtracted integrated activity images (Fig. 4). If the subtraction is complete, the image value in the chamber could only be due to the spillover (from the myocardium). The ratio should be the same on images with or without decay correction, because the spillover fraction is only related to the image resolution and the shape of the cross section. On the other hand, if blood-pool activity is incompletely subtracted, the chamber to myocardium activity ratio for the decay-corrected image would be lower than that for the nondecay-corrected image, because the integrated decay-corrected radioactivity relative to the nondecay-corrected integral is lower in blood than in myocardium. The reverse is true if the blood pool is over subtracted.

Even if the position and the geometry of the cross section remain constant, direct subtraction does not always remove blood-pool activity contributions com-

pletely. This is shown by the relatively higher value in right ventricle of the ^{15}O water image (Fig. 3) than in the chamber of the right ventricle of the ^{15}O CO image (Fig. 1). This is caused by the transit time delay of ^{15}O water from the right ventricle to the left ventricle after the tracer has been introduced intravenously. Because of the short half-life of ^{15}O , a transit time delay of about 8 sec would affect the time integral of the nondecay-corrected activity by about 5%. Since the blood-pool subtraction is based on the arterial blood concentrations [Eq. (1)], the subtraction removes the blood-pool activity in the left ventricle quite completely, but leaves some residues in the right ventricle of the integral image of the nondecay corrected activity. Incomplete removal could result in a much larger percent error in myocardium, because the amount of the time integrated nondecay-corrected radioactivity in myocardium is smaller than in the cardiac chambers. This leads to larger values of the calculated MBF in the interventricular septum which is adjacent to the right ventricle. This most likely explains why the technique overestimated MBF in the interventricular septum in two studies listed in Table 1 (D475R1 and R2).

Quantitative values of MBF and distribution volume

As shown in Fig. 6, MBF measured by ^{15}O water correlates well with the MBF by the microsphere technique over the flow range studied, although a systematic underestimation is noted.

The partial volume effect (17) primarily accounts for this underestimation. The effect can be corrected for if the object configuration is known. However, the major goal of the present study was to examine the technical feasibility of the ^{15}O water and positron CT technique for in vivo measurement of MBF. We selected the

TABLE 2
Comparison of Blood Curve Integrals with Those from Blood Pool in Positron CT Images

| Study no. | From blood samples | | | From positron images | | | | Normalized* blood-pool activity | $\frac{\int Q_b^* dt / \int Q_b dt}{\int C_i^* dt / \int C_i dt}$ |
|-----------|--------------------|-----------------|-------------------------------------|----------------------|-----------------|-------------------------------------|-----------------------------------|---------------------------------|---|
| | $\int C_i dt$ | $\int C_i^* dt$ | $\frac{\int C_i^* dt}{\int C_i dt}$ | $\int Q_b dt$ | $\int Q_b^* dt$ | $\frac{\int Q_b^* dt}{\int Q_b dt}$ | $\frac{\int Q_b dt}{\int C_i dt}$ | | |
| D407R1 | 11.27 [†] | 25.21 | 2.24 | 8.46 | 20.21 | 2.39 | 0.75 | 0.63 | 1.07 |
| D451R1 | 5.78 | 20.14 | 3.48 | 5.17 | 18.86 | 3.65 | 0.89 | 0.81 | 1.05 |
| D451R2 | 8.53 | 24.73 | 2.90 | 6.65 | 21.01 | 3.16 | 0.79 | 0.81 | 1.10 |
| D455R1 | 8.06 | 25.15 | 3.12 | 7.86 | 27.78 | 3.53 | 0.97 | 0.82 | 1.13 |
| D457R1 | 5.95 | 19.02 | 3.20 | 5.82 | 18.91 | 3.25 | 0.98 | 0.90 | 1.02 |
| D457R2 | 3.79 | 11.49 | 2.95 | 3.51 | 10.80 | 3.08 | 0.93 | 0.90 | 1.04 |
| D460R2 | 2.66 | 8.74 | 3.29 | 2.42 | 8.21 | 3.39 | 0.91 | 0.79 | 1.03 |
| D475R1 | 3.07 | 9.40 | 3.06 | 2.74 | 8.53 | 3.39 | 0.89 | 0.84 | 1.02 |
| D475R2 | 4.32 | 12.12 | 2.81 | 3.67 | 10.73 | 2.92 | 0.85 | 0.84 | 1.04 |
| D495R1 | 13.16 | 48.59 | 3.69 | 11.80 | 45.26 | 3.84 | 0.90 | 0.87 | 1.04 |
| D495R2 | 12.01 | 42.59 | 3.55 | 10.66 | 38.74 | 3.63 | 0.89 | 0.87 | 1.02 |
| D495R3 | 6.96 | 28.16 | 4.04 | 6.20 | 25.60 | 4.13 | 0.89 | 0.87 | 1.02 |

* The ratio of measured radioactivity concentrations by positron CT and arterial blood samples during ¹⁵O CO study.

[†] Values of $\int C_i dt$, $\int C_i^* dt$, $\int Q_b dt$ and $\int Q_b^* dt$ are in arbitrary units, but are directly comparable within study.

closed-chest dog model in order to simulate conditions for human studies. Matching the in vitro heart slice with the cross section scanned by positron CT is difficult in the closed-chest animal. Also, the left ventricular geometry probably changed from the in vitro to the ex vivo condition, not to mention effects of cardiac motion which were not eliminated because the NeuroECAT has no gating capacity. These uncertainties made corrections for partial volume effect difficult, and could account for the large scatter of the data. Nevertheless, by considering the image resolution of 1.2 cm FWHM and the approximate wall thickness of 1.0 cm for left ventricular myocardium, the recovery coefficient (17) due to the partial volume effect is about 0.7, which is not inconsistent with the slope of the relationship shown in Fig. 6 between MBF determined in vivo by positron CT and the in vitro values by the microsphere technique. Although the finite permeability of water in crossing the capillary wall (13,31) could also cause underestimation for MBF by positron CT, its effect, which is flow dependent (32,33), is not clearly evident over the flow range covered in this study.

The difficulties in matching the results of the two techniques, the ¹⁵O water and the microsphere techniques, are major sources of the data scatter in Fig. 6. In addition to the configurational changes and the mismatch in cross sections as discussed above, variations in MBF between the injection times of microsphere and ¹⁵O water (separated by about 4 min) may also account for the scatter in the data. If these difficulties are solved, the correlation between the results of the two techniques is expected to be better. However, the ¹⁵O water technique is quite susceptible to errors and further validation of its accuracy is needed.

Contrary to the relatively large variability of the calculated MBF, the calculated distribution volume of water is more constant, and the image of distribution volume is less noisy than the MBF image. The obtained distribution volume value of 0.74 ml/g is lower than the value of 0.82 ml/g for the brain (10), as expected from consideration of the partial volume effect. However, the usefulness of the myocardial water distribution volume for indicating myocardial abnormality is unclear.

CONCLUSION

In the present study, the use of ¹⁵O water and positron CT for quantitative measurement of MBF has been investigated. Several potential difficulties associated with dynamic study of myocardial tracers with positron CT have been discussed. The results support the feasibility of the technique for measurement of MBF in absolute units. Oxygen-15-labeled water for measurement of MBF has many desirable features. For example, measurements can be repeated quickly (within 10–15 min); the radiation burden to the patient is low (because of the short half-life); the measurement is relatively unaffected by other physiological processes (unlike [¹³N]ammonia, rubidium-82, or other potassium analogs); the study can be used in conjunction with ¹⁵O oxygen to measure oxygen utilization [as demonstrated by Frackowiak et al.'s elegant studies in the brain (8)]. While many technical aspects await further improvement and the accuracy of the approach needs to be defined more clearly, our results indicate that the technique merits further investigation. Development of advanced positron CT scanners of better spatial and temporal resolutions (34) will definitely alleviate some of the technical dif-

ficulties like cardiac gating, partial volume effect, and spillover from cardiac chambers. The larger size of the human heart is also expected to reduce several of the limitations encountered in this study in canine myocardium and result in better and more reliable measurements.

ACKNOWLEDGMENTS

This work was supported by DOE contract DE-AM03-76-SF-0012, NIH Grants R01-HL-29845, R01-HL-30673, R01-GM-24839-01, Group Investigatorship Award 617 IG by the Greater Los Angeles Affiliate of the American Heart Association, and donations from Jennifer Jones/Simon Foundation, and Ahmanson Foundation, Los Angeles, CA.

The authors would like to thank the UCLA medical cyclotron staff for production of ^{15}O water and ^{15}O CO used in the study; Ron Sumida, Larry Pang, and Francine Aquilar for carrying out the positron CT scanning; Tony Ricci, Philippe Collard, and Rachel Schwab for computer hardware and software support; and Lee Griswold for illustrations.

FOOTNOTES

† NeuroECAT is a registered trademark of Computer Technology & Imaging, 215 Center Park Drive, Knoxville, TN 37922.

‡ Cyclotron Corp., Berkeley, CA.

§ Series 500 Biotronix, Silver Springs, MD.

¶ Brush 200, Gould Inc., Cleveland, OH.

** 3M Company, Minneapolis, MN.

REFERENCES

- Phelps ME: Emission computed tomography. *Semin Nucl Med* 7:337-365, 1977
- Phelps ME, Mazziotta JC, Huang SC: Study of cerebral function with positron computed tomography. *J Cereb Blood Flow Metab* 2:113-162, 1982
- Huang SC, Carson RE, Phelps ME: Tracer kinetic modeling in positron computed tomography. In *Tracer Kinetics and Physiologic Modeling*, Lambrecht RM, Rescigno A, eds. New York, Springer-Verlag, 1983, pp 298-344
- Schelbert HR, Phelps ME, Hoffman EJ, et al: Regional myocardial perfusion assessed by N-13 labeled ammonia and positron emission computerized axial tomography. *Am J Cardiol* 43:208-218, 1979
- Schelbert HR, Wisenberg G, Phelps ME, et al: Non-invasive assessment of coronary stenosis by myocardial imaging during pharmacologic vasodilation. VI. Detection of coronary artery disease in man with intravenous N-13 ammonia and positron computed tomography. *Am J Cardiol* 49:1197-1207, 1982
- Shah A, Schelbert HR, Schwaiger M, et al: Noninvasive measurement of regional myocardial blood flow with N-13 ammonia and positron computed tomography in intact dogs. *J Am Coll Cardiol* 5:92-100, 1985
- Bergmann ST, Hack S, Tewson T, et al: The dependence of accumulation of $^{13}\text{NH}_3$ by myocardium on metabolic factors and its implications for the quantitative assessment of perfusion. *Circulation* 61:34, 1980
- Frackowiak RSJ, Lenzi G-L, Jones T, et al: Quantitative measurement of regional cerebral blood flow and oxygen metabolism in man using O-15 and positron emission tomography: Theory, procedure, and normal values. *J Comput Assist Tomogr* 4:727-736, 1980
- Frackowiak RSJ, Pozzilli C, Legg NJ, et al: Regional cerebral oxygen supply and utilization in dementia: A clinical and physiological study with oxygen-15 and positron tomography. *Brain* 104:753-778, 1981
- Huang SC, Carson RE, Hoffman EJ, et al: Quantitative measurement of local cerebral blood flow in humans by positron computed tomography and ^{15}O -water. *J Cereb Blood Flow Metab* 3:141-153, 1983
- Raichle ME, Martin WRW, Herscovitch P, et al: Brain blood flow measured with intravenous H_2^{15}O . II. Implementation and validation. *J Nucl Med* 24:790-798, 1983
- Alpert MM, Ackerman RH, Correia JA, et al: Measurement of rCBF and rCMRO₂ by continuous inhalation of ^{15}O -labeled CO₂ and O₂. *Acta Neurol Scand* 56(Suppl 72):186-187, 1977
- Yipintsoi T, Bassingthwaigite JB: Circulatory transport of iodoantipyrine and water in the isolated dog heart. *Circ Res* 27:461-477, 1970
- Bergmann SR, Fox KAA, Rand AL, et al: Quantification of regional myocardial blood flow in vivo with H_2^{15}O . *Circulation* 70:724-733, 1984
- Allan RM, Jones T, Rhodes CCG, et al: Quantitation of myocardial perfusion in man using oxygen-15 and positron tomography. *Am J Cardiol* 47:481, 1981 (abstr)
- Jones T, Chesler DA, Ter Pogossian MM: The continuous inhalation of oxygen-15 for assessing regional oxygen extraction in the brain of man. *Br J Radiol* 49:339-343, 1976
- Hoffman EJ, Huang SC, Phelps ME: Quantitation in positron emission tomography. 1. Effect of object size. *J Comput Assist Tomogr* 3:299-308, 1979
- Wisenberg G, Schelbert HR, Hoffman EJ, et al: In vivo quantitation of regional myocardial blood flow by positron-emission computed tomography. *Circulation* 63:1248-1258, 1981
- Henze E, Huang SC, Ratib O, et al: Measurements of regional tissue and blood-pool radiotracer concentrations from serial tomographic images of the heart. *J Nucl Med* 24:987-996, 1983
- Hoffman EJ, Phelps ME, Huang SC: Performance evaluation of a positron tomograph designed for brain imaging. *J Nucl Med* 24:245-257, 1983
- Ricci AR, Hoffman EJ, Phelps ME, et al: Investigation of a technique for providing a pseudo-continuous detector ring for positron tomography. *IEEE Trans Nucl Sci* NS-29:452-456, 1982
- Hoffman EJ, Ricci AR, Van Der Stee LMAM, et al: ECAT III—basic design considerations. *IEEE Trans Nucl Sci* NS-30:729-733, 1983
- Huang SC, Carson RE, Phelps ME: Measurement of local blood flow and distribution volume with short-lived isotopes: A general input technique. *J Cereb Blood Flow Metab* 2:99-108, 1982
- Heymann MA, Payne BD, Hoffman JIE, et al: Blood flow measurements with radionuclide-labeled particles. *Prog Cardiovasc Dis* 20:55-79, 1977
- Schelbert HR, Phelps ME, Huang SC, et al: N-13 ammonia as an indicator of myocardial blood flow. *Circulation* 63:1259-1272, 1981
- Phelps ME, Huang SC, Hoffman EJ, et al: Tomographic

- measurement of local cerebral glucose metabolic rate in man with 2-(F-18)fluoro-2-deoxy-D-glucose, *Ann Neurol* 6:371-388, 1979
27. Huang SC, Phelps ME, Hoffman EJ, et al: Noninvasive determination of local cerebral metabolic rate of glucose in man. *Am J Physiol* 238:E69-E82, 1980
 28. Bard Y: *Nonlinear Parameter Estimation*, New York, Academic Press, 1974
 29. Bergmann SR, Fox KAA, Collen D, et al: Coronary thrombolysis achieved with human extrinsic plasminogen activator, a clot selective activator, administered intravenously. *J Am Coll Cardiol* 1:615, 1983 (abstr)
 30. Frank JS, Langer GA: The myocardial interstitium: Its structure and its role in ionic exchange. *J Cell Biol* 6: 586-601, 1974
 31. Rose CP, Goresky CA, Bach GG: The capillary and sarcolemmal barriers in the heart: An exploration of labeled water permeability. *Circ Res* 41:515-533, 1977
 32. Renkin EM: Transport of potassium-42 from blood to tissue in isolated mammalian skeletal muscles. *Am J Physiol* 197:1205-1210, 1959
 33. Crone C: Permeability of capillaries in various organs as determined by use of the indicator diffusion method. *Acta Physiol Scan* 58:292-305, 1964
 34. Phelps ME, Huang SC, Hoffman EJ, et al: An analysis of signal amplification using small detectors in positron emission tomography. *J Comput Assist Tomogr* 6: 551-565, 1982